


Article

# Influence of Wall Heat Effect on Gas Explosion and Its Propagation

Zhenzhen Jia <sup>\*</sup>, Qing Ye and Zhuohua Yang

School of Resource, Environment and Safety Engineering, Hunan University of Science and Technology, Xiangtan 411201, China; cumtyeqing@126.com (Q.Y.)

\* Correspondence: jiazhenzhen1982@126.com

**Abstract:** The gas explosion process in pipes is often accompanied by an intense wall heat effect. A considerable part of the explosion energy is dissipated, and the process of gas explosion and its propagation is affected. In order to study the influence of wall heat effect on gas explosion and its propagation, numerical models of gas explosion in pipes with different adiabatic degrees were established by ANSYS/LS-DYNA. The propagation process of gas explosion in pipes under the influence of the wall heat effect was numerically simulated and analyzed, and the thermal stress and temperature distribution of pipes with different adiabatic degrees were studied. The results show that with a decrease in pipe insulation, the wall heat effect increases, the heat loss of gas explosion increases, and the overpressurization of the shock wave, the explosion intensity, and the thermal stress of the pipe wall are significantly reduced. The results indicate that the wall heat effect can weaken the gas explosion and its propagation. At the same time, it is found that the influence of the wall heat effect on the initiation section is greater than that on other positions of the pipe. With the decrease in the heat effect of the pipe wall, the heat loss of the wall decreases, the temperature difference between the inner and outer wall surfaces expands, and the total energy released by the gas explosion increases. The released energy is used to heat and compress the unburned gas, resulting in a more intense explosion reaction and a substantial increase in the temperature of the explosive gas. Therefore, it can be seen that the wall heat effect has an important influence on the gas explosion and its propagation. The influence of wall adiabatic condition on gas explosion with a higher combustion level is greater than the influence on gas explosion with low combustion levels.



**Citation:** Jia, Z.; Ye, Q.; Yang, Z.

Influence of Wall Heat Effect on Gas Explosion and Its Propagation.

*Processes* **2023**, *11*, 1326.

<https://doi.org/10.3390/pr11051326>

Academic Editor: Maria Mitu

Received: 22 March 2023

Revised: 17 April 2023

Accepted: 20 April 2023

Published: 25 April 2023



**Copyright:** © 2023 by the authors. Licensee MDPI, Basel, Switzerland. This article is an open access article distributed under the terms and conditions of the Creative Commons Attribution (CC BY) license (<https://creativecommons.org/licenses/by/4.0/>).

**Keywords:** gas explosion; heat loss; wall heat effect; numerical simulation

## 1. Introduction

It is wellknown that a gas explosion will radiate and transfer some heat to the surrounding, reduce the energy involved in the explosion reaction, and affect the gas explosion and its propagation. The gas state parameters change dramatically, especially gas explosions in confined spaces with high temperature and pressure, such as a gas explosion in a pipe [1]. The energy released by the chemical reaction generated by the intense heat and mass exchange between the unburned gas mixture and the flame front supports the flame to push forward continuously [2]. The flame propagation acceleration will be weakened, and even the flame will be extinguished if the heat loss of the wall consumes the energy released by the chemical reactions at this time [3–6]. Since the gas explosion is a reaction with high temperature and high pressure, there is a huge temperature difference between the inner and outer walls of the pipe. At this time, the heat released during the explosion will be transferred to the wall and released to the external environment. Thus the heat energy that is heating and compressing the unburned gas body is reduced, and the intensity of the reaction is reduced [7].

Since the heat loss of the wall is an important factor affecting the gas explosion and its propagation, many scholars take into account the influence of the wall heat effect on a gas

explosion. Zhang et al. carried out gas explosion experiments with spherical containers [8]. It is found that the explosion overpressurization of the end wall ignition is 40% lower than that in the central ignition case, and the lower flame velocity and larger contact area with the wall at the initial phase can cause more wall heat loss and reduce the intensity of the gas explosion. Junchun Zhang et al. investigated the inclined flame front break in the filtration gas combustion of a lean methane ( $\text{CH}_4$ )/air mixture during propagation downstream in an inert porous medium by a two-temperature and two-dimensional numerical model [9]. Results show that the flame front break easily takes place in larger wall heat loss, higher Lewis number mixtures, higher inlet velocity, and lower equivalence ratio regimes. Tao Wang et al. investigated the explosion thermal behavior of  $\text{H}_2/\text{CH}_4$ /air in a confined 20 L vessel and obtained the volume ratios with the highest or lowest combustion heat loss [10]. Gao et al. conducted low-concentration coal mine methane (LCM) combustion experiments and revised numerical models [11,12], results indicated that the temperature distribution exhibits a one-dimensional nature evidently with the adiabatic wall, but the temperature discrepancy is apparent when the heat loss of the wall is considered. Wang et al. investigated the explosion behaviors of syngas-air mixtures in a vessel with a large blockage ratio perforated plate [13]. It was found that both the perforated plate and the vessel wall caused heat loss and reduced the maximum explosion pressure, and the closer the perforated plate was to the ignition position, the more serious the heat loss was and the smaller the explosion pressure was. In addition, increasing the turbulence intensity of combustible gas in the vessel can weaken the wall heat effect and reduce the heat loss through the vessel wall [14,15]. In order to study the wall heat effect of the roadway in the gas explosion process, the temperature variation of the flame wave of gas explosion was studied [16,17]. Based on the mathematical formula of heat conduction, the influencing factors, such as convective heat-transfer coefficient, flame temperature, and heat duration of the flame wave, were analyzed and calculated in combination with these experimental data. Ye et al. studied the influence of the wall heat effect on the propagation characteristics of gas explosion by experiments from the perspective of the energy change characteristics of explosion wave. It is considered that the heat release of an explosion can be divided into wall heat dissipation, unburned gas preheating, explosion wave energy, product kinetic energy, and other losses during propagation [18].

Generally, the experimental investigation on roadway gas explosion is conducted in a pipe experiment system. For the sake of safety, steel pipes with higher pressure resistance and wall thickness are often used in experimental piping [19–21]. The good thermal conductivity of steel pipes and the high heat capacity due to the large wall thickness will make the heat loss on the wall more obvious [22]. A.N. Campbell carried out a numerical study of thermal explosion in a spherical reactor under the influence of natural convection and external heat transfer, presented that the existence of these additional heat transfer resistances on the wall may alter the rate of heat transfer from the hot region in the reactor to the environment and hence change the stability of the reaction [23]. Yunfei Yan et al. studied the influence of different wall materials on gas combustion characteristics by numerical simulation method and found that reducing the thermal conductivity of the wall can significantly increase the hot spots and temperature in the reaction zone [24]. It can be inferred that the wall heat loss or wall heat effect will vary with the thermal properties of the wall. In fact, gas explosion accidents often occur in places such as underground roadways, where the wall thermal conductivity is poor, as shown in Table 1, and the wall heat loss has little effect on a gas explosion. It can be inferred that there is a certain gap between the results in the laboratory and the actual situation. In order to better apply the existing research results to the actual safety production, it is necessary to study the influence of the wall heat effect on the gas explosion process. In our previous research [25], the influence of a pipe's wall heat effect on gas explosion and its propagation is theoretically analyzed mainly from perspectives of the heat transportation and reaction process. The experimental results verified the significant influence of wall heat loss on gas explosion strength. However, as in many previous studies, the experimental studies only discussed the properties of flame

and shock waves and were unable to analyze the detailed energy changes and temperature flow fields at the wall. This made it difficult to specifically examine the effect of wall heat effects on gas explosions. Therefore, this study presents a numerical simulation of the influence of the wall heat effect on gas explosion and its propagation process. The changes in thermal stress, energy transfer, and temperature field in the gas explosion process are analyzed specifically. The results are of great practical significance for improving the theory of the wall heat effect and enhancing the prevention and control level of gas explosions in confined spaces.

**Table 1.** Thermal properties of underground roadway wall.

Lithology	Heat Capacity J/(kg·°C)	Thermal Conductivity W/(m·°C)
Sandstone	840	1.84
Coal	1050	0.17
Shale	775	1.72
Mudstone	922	2.73
Limestone	908	2.09
Steel	460	45

## 2. Numerical Model

### 2.1. Mathematical Model

The propagation of gas explosion in a pipe is a continuous process of releasing and consuming energy. The energy released by a gas explosion does work by expanding and expanding pressure waves constantly superimpose on the explosion wavefront. When the supplementary energy of the explosion wavefront is greater than the consumed energy, the intensity of the explosion wave increases, and vice versa. If the supplementary energy is equal to the consumed energy, the intensity of the explosion wave remains unchanged. The energy equation on both sides of the explosion wavefront can be expressed as follows [25]:

$$Q + e_1 + \frac{p_1}{\rho_1} + \frac{(D_f - u_1)^2}{2} = e_2 + \frac{p_2}{\rho_2} + \frac{(D_f - u_2)^2}{2} \quad (1)$$

where,  $Q$  is the released energy in the combustion reaction;  $e_1$ ,  $e_2$  are the specific internal energy;  $p$  is the pressure;  $D_f$  is the velocity of explosion wave;  $\rho_1$ ,  $\rho_2$  are the density of gas;  $u_1$ ,  $u_2$  are the flow velocity on both sides of the flame front.

In the propagation process of a gas explosion, the explosion releases heat, and the temperature and enthalpy of the burned high-temperature combustion product increase, then turn into the energy of the explosion wave and kinetic energy of products by expansion [26]. Due to the temperature difference, the incandescent high-temperature combustion products dissipate heat to the wall by convection and thermal radiation and transmit heat to the unburned gas by thermal conduction, diffusion, and thermal radiation. The propagation of gas explosion in a pipe is usually assumed to be one-dimensional to derive its energy balance equation, as shown in Figure 1. The flame wavefront moves forward  $dx_1$  and releases heat  $\delta Q$  in time  $d\tau$ . During this process, the pipe wall dissipates heat  $\delta Q_1$  from convection and thermal radiation, and transfers heat  $\delta Q_2$  to the unburned gas through thermal conduction, thermal radiation, and diffusion, and the shock wavefront moves forward  $dx_2$  in the same time. The energy balance equation can be obtained as follows:

$$\delta Q = \delta Q_1 + \delta Q_2 + dE_s + dE_k + dR_m \quad (2)$$

where,  $dE_s$  is the energy change of an explosion wave (shock wave) in the infinitesimal time, namely the energy increment of compressed gas,  $dE_k$  is the energy increment of the burned gas in the infinitesimal time,  $dR_m$  is the energy loss in infinitesimal time.

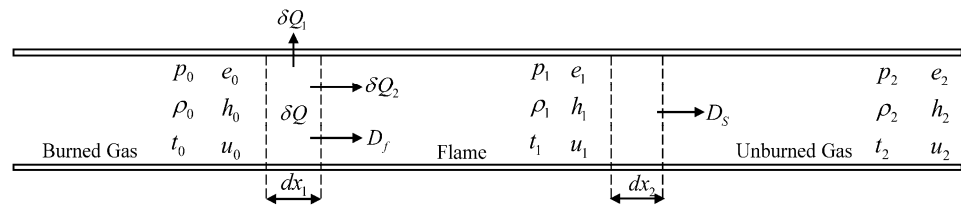


**Figure 1.** The sketch of energy equilibrium of gas explosion in a pipe.

Referring to the previous experimental study results on the wall heat effect of gas explosion in pipes [25], thermal-solid coupling models of gas explosion in pipes are established by ANSYS/LS-DYNA in this study, and the numerical models are verified through experimental data. On this basis, numerical simulation is carried out to obtain some data and phenomena that are difficult to obtain in experiments.

In the LS-DYNA solver, while using a Cartesian coordinate system, the basic governing equations (mass, momentum, and energy equation) for the three-dimensional unsteady flow in a gas explosion can be expressed as follows [25,27].

The mass conservation equation is given by:

$$\frac{\partial \rho}{\partial t} + \frac{\partial(\rho u)}{\partial x} + \frac{\partial(\rho v)}{\partial y} + \frac{\partial(\rho w)}{\partial z} = 0 \quad (3)$$

The momentum conservation equation is given by:

$$\begin{cases} \frac{\partial u}{\partial t} + u \frac{\partial u}{\partial x} + v \frac{\partial u}{\partial y} + w \frac{\partial u}{\partial z} = -\frac{1}{\rho} \frac{\partial \rho}{\partial x} \\ \frac{\partial v}{\partial t} + u \frac{\partial v}{\partial x} + v \frac{\partial v}{\partial y} + w \frac{\partial v}{\partial z} = -\frac{1}{\rho} \frac{\partial \rho}{\partial y} \\ \frac{\partial w}{\partial t} + u \frac{\partial w}{\partial x} + v \frac{\partial w}{\partial y} + w \frac{\partial w}{\partial z} = -\frac{1}{\rho} \frac{\partial \rho}{\partial z} \end{cases} \quad (4)$$

The energy conservation equation is given by:

$$\frac{\partial e}{\partial t} + u \frac{\partial e}{\partial x} + v \frac{\partial e}{\partial y} + w \frac{\partial e}{\partial z} = 0 \quad (5)$$

Where,  $x$ ,  $y$ , and  $z$  are coordinate parameters,  $m$ ;  $t$  is the time coordinate,  $s$ ;  $u$ ,  $v$ , and  $w$  are the velocities in three coordinate directions, respectively,  $m/s$ ;  $\rho$  is the density of fluid,  $kg/m^3$ .

The differential equations of heat conduction in a three-dimensional continuum model are given by:

$$\rho c_p \frac{\partial \theta}{\partial t} = (k_{ij} \theta_{,j})_{,i} + Q \quad (6)$$

Subject to the boundary conditions:

$$\theta = \theta_i \text{ on boundary } \Gamma_1 \quad (7)$$

$$k_i \theta_{,j} \cdot \eta_i + \beta \theta = \gamma \text{ on boundary } \Gamma_2 \quad (8)$$

And initial conditions at  $t_0$ :

$$\theta_{\Gamma} = \theta_0(x_i) \text{ at } t = t_0 \quad (9)$$

where,  $\theta = \theta(x_i, t)$  is the temperature at  $t$  on  $x_i$ , K;  $x_i = x_i(t)$  is the coordinates as a function of time;  $\rho = \rho(x_i)$  is the density,  $kg/m^3$ ;  $c_x = c_x(x_i, \theta)$  is the specific heat;  $x_y = k_y(x_i, \theta)$  is the thermal conductivity,  $W/m \cdot K$ ;  $Q = Q(x_i, \theta)$  is the internal heat generation rate per unit volume  $\Omega$ ,  $W/m^3$ ;  $\theta_{\Gamma}$  is the prescribed temperature on  $\Gamma_1$ , K;  $n_i$  is the normal vector to  $\Gamma_2$ .

## 2.2. Numerical Model and Fundamental Assumptions

The geometric size of the model is shown in Figure 2. The rectangular pipe with a length of 4 m, where the ignition part is closed, and the end is open. The inner diameter is 80 mm, and the pipe wall thickness is 12 mm. The asbestos cloth with a large specific heat capacity and small thermal conductivity of 0.8 mm thickness is used as an adiabatic layer, which is attached to the inner wall surface of the pipe. The adiabatic degree of the pipe is changed to study the influence of wall heat effect on pipe gas explosion. According to the length of the asbestos cloth in the pipe, the influence of the wall heat effect is distinguished. Three numerical simulations are carried out for the non-adiabatic pipe (without the adiabatic layer in the pipe, and the wall heat effect is the most serious), semi-adiabatic pipe (with 2 m adiabatic layer at the initiation section of the pipe, the wall heat effect is relatively serious) and adiabatic pipe (with 4 m adiabatic layer in the pipe, the wall heat effect is the weakest).

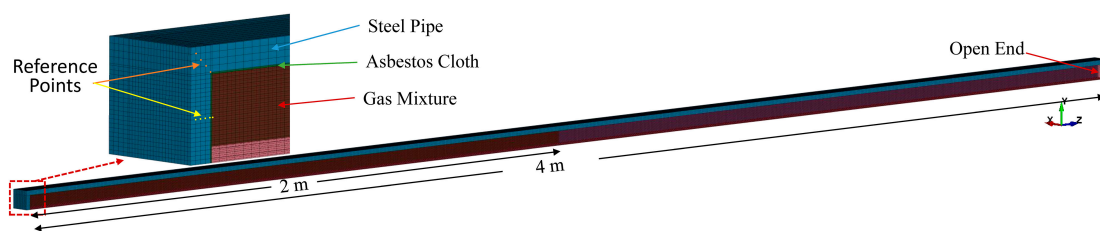


**Figure 2.** Schematic diagram of the numerical model of pipe.

Figure 2 shows the size and mesh of the numerical model. A 1/4 model is used to reduce the computational cost. The model is divided into three parts, namely, gas mixture, steel pipe, and adiabatic layer (asbestos cloth), which are connected by the common-node and thermal-solid coupling method. The model is meshed by Solid164, and the mesh number in x, y, and z directions is 24, 24, and 804, respectively (non-adiabatic model), while adding an adiabatic layer it is 25, 25, and 805 (semi-adiabatic model and adiabatic model), so the total number of meshes is 463,104 and 503,125, respectively. The symmetry constraint is set on the symmetry plane. The axial constraint is set on the opening end of the pipe to prevent abnormal deformation of the pipe, and the non-reflecting boundary is set on the gas boundary at the opening end. The initial temperature of the model is set to 20 °C. In order to simulate the heat exchange between the pipe and the external environment in the process of a gas explosion, the ambient temperature boundary is set on the outer wall surface of a pipe.

In order to simplify the model and make it realistic, the following assumptions were made in the numerical simulation:

- (1) The local ambient temperature is 20 °C and the ambient pressure is  $1.01 \times 10^5$  Pa;
- (2) The pipe is filled with a pre-mixed ideal gas at the initial time, with a gas concentration of 9.5%;
- (3) The explosion initiation time is at 0 s, and the initiation point is at 0.05 m from the closed end;
- (4) Gravity is not considered;
- (5) The steel pipe and the asbestos layer are smooth, isotropic, and ideal-elastic materials, which have not been damaged during the explosion;
- (6) A gas explosion is a chemical reaction with a very rapid reaction, and a large number of intermediate and instantaneous products are produced in the process of explosion. In this paper, only one step reaction of the gas explosion is considered. Namely, in reaction,  $\text{CH}_4 + \text{O}_2 = \text{CO}_2 + \text{H}_2\text{O}$  is only considered. Intermediates and instantaneous products are not considered.

### 2.3. Material Model and Parameters

The TNT equivalent method is used to simulate the explosion source. The converted explosion source is divided into five parts, equally distributed on the pipe axis, and experimental data are used to correct the parameters of each explosion source. The pipe in the gas explosion experiment is always good in anti-explosion performance, and there is no deformation after an experiment. The focus of this study is the heat transfer relationship in the process of a gas explosion. Therefore, the isotropic thermo-elastic material models are used for steel pipes and asbestos, which are defined by \*MAT\_ELASTIC and \*MAT\_THERMAL\_ISOTROPIC. The material model has high computational efficiency and can better simulate the heat exchange and temperature distribution between gas and pipe walls in the process of a gas explosion. The specific parameters of the material are shown in Table 2.

**Table 2.** Parameters of material model.

	$\rho$ kg/m <sup>3</sup>	$E$ GPa	Heat Capacity J/(kg·°C)	Thermal Conductivity W/(m·°C)
Steel Pipe	7980	2.07	460	45
Asbestos Cloth	1000	0.013	840	0.46

## 3. Results and Discussion

### 3.1. Verification and Validation of the Numerical Model

In order to ensure the accuracy of the numerical model, it is necessary to verify the mesh independence and time-step independence [28], as shown in Figure 3. The results of five numerical models (non-adiabatic model) with mesh numbers on the order of  $9 \times 10^4$ ,  $16 \times 10^4$ ,  $32 \times 10^4$ ,  $46 \times 10^4$ , and  $54 \times 10^4$  are compared. It is found that the results of  $46 \times 10^4$  and  $54 \times 10^4$  are very close, indicating that the mesh number in the order of  $46 \times 10^4$  can meet the mesh independence and no densification is required, so the mesh number is set as 463,104. For the verification of time-step independence, it is found that the difference between the results of  $1 \times 10^{-4}$  s and  $5 \times 10^{-5}$  s is very small, so  $1 \times 10^{-4}$  s is selected as the time step size of the model.

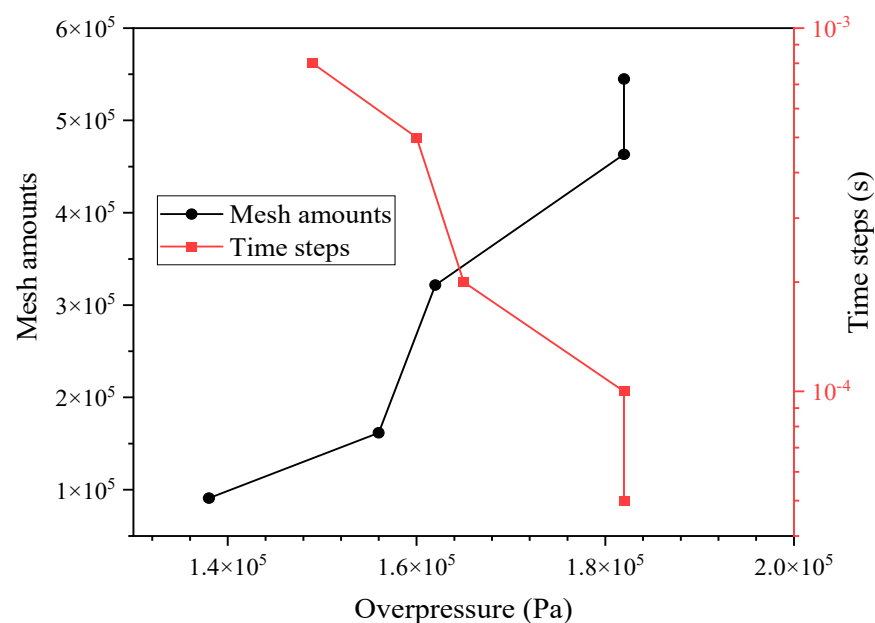


**Figure 3.** Verification of mesh independence and time-step independence.

On the basis of independent verification, the numerical model is optimized, and the simulation results are compared with the experimental results, as shown in Figure 4. As

can be seen, a good match can be obtained between the simulation results in this paper and the reported results in the experimental study, and the error mainly occurs at  $L/D = 22$ . The reason may be that the friction of the pipe wall in the experiment leads to a part of the energy dissipation of the gas explosion. In the numerical simulation, the pipe is ideally smooth, and this part of the energy dissipation is not calculated [29–31]. The error of the numerical model is very small, so it has enough reliability to carry out this study.

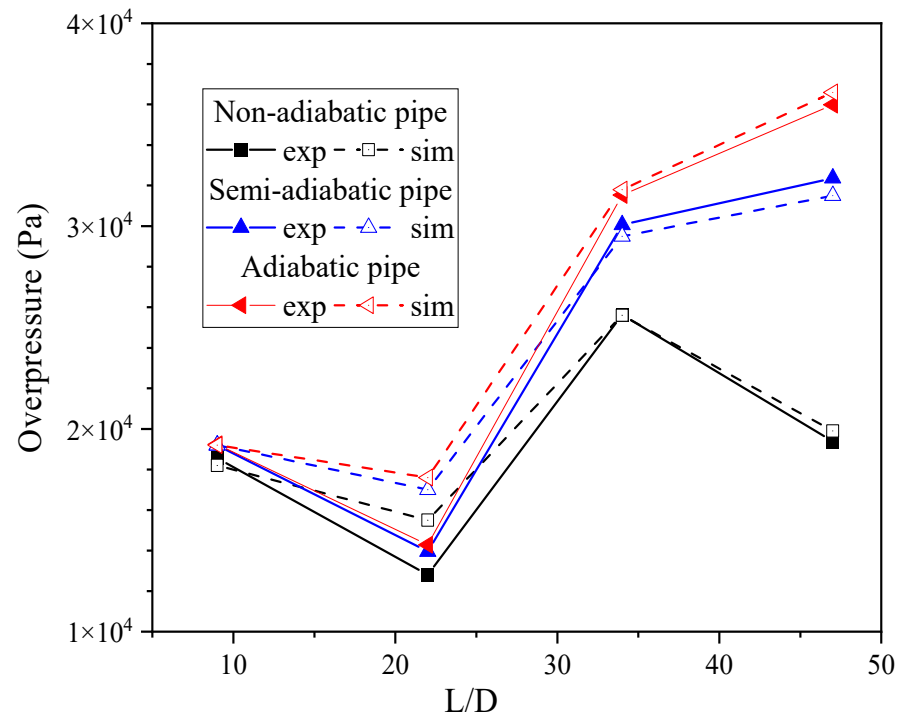


**Figure 4.** Verification of simulation results with experimental data.

### 3.2. Influence of Wall Heat Effect on the Gas Explosion Propagation

Figures 5 and 6 show the overpressure variation during the propagation of gas explosion in pipes. As shown in Figure 5, the intensity of the gas explosion is weak, and the propagation speed is slow in the initial phase of the explosion. With the subsequent chemical reaction, the intensity of the explosion increases continuously, and the propagation of the high-pressure wave front continues to accelerate. At about 13.8 ms, the explosion wave reaches the open end of the pipe, and the explosion reaction process is basically finished. Then the explosion wave and flame spread into the air, and the pressure in the pipe continues to drop until it reaches the atmospheric pressure. Figure 6a is a detailed comparison of the overpressure variation at different locations of the pipe. With the distance increase from the initiation point, the arrival time of the explosion wave is delayed, and the maximum overpressure shows a decreasing-increasing-decreasing pattern, which is consistent with the experimental results in reference. In Figure 6b, the maximum overpressure of the explosion wave increases obviously with the decrease in the wall heat effect, and the maximum overpressure of the gas explosion increases by 15.2% and 24.2% with the decrease in the wall heat effect. The wall heat effect at the initiation section of the pipe has the most obvious effect on the intensity of the gas explosion, and reducing the wall heat effect at the latter half of the pipe can also increase the intensity of the gas explosion. As can be seen from Figure 6, there are much clutter and vibration, which may be caused by wall shock wave reflection.

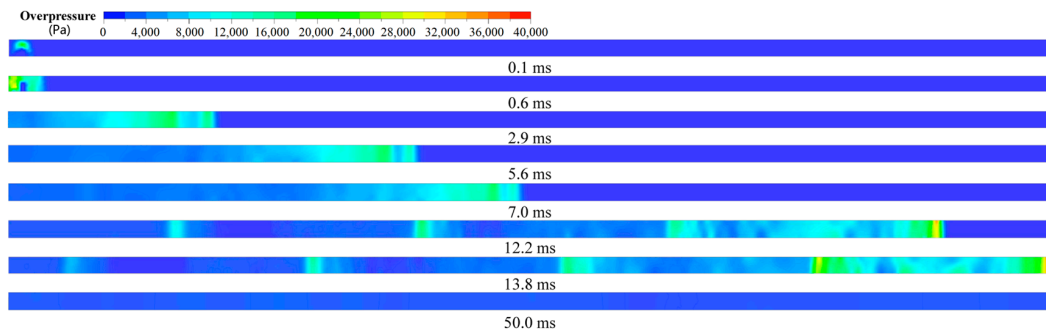
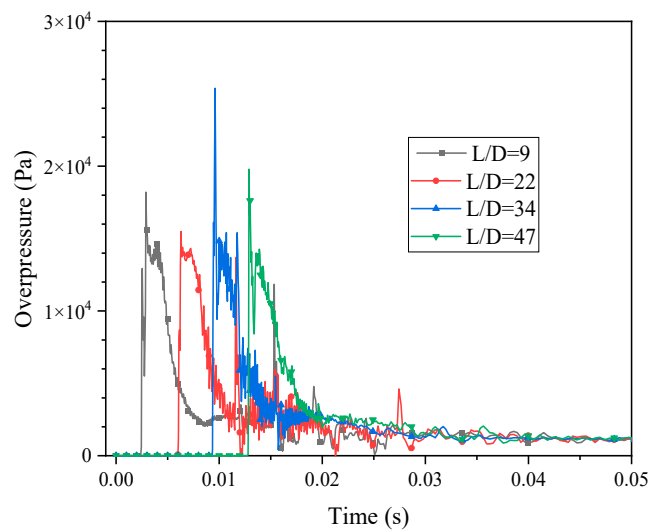
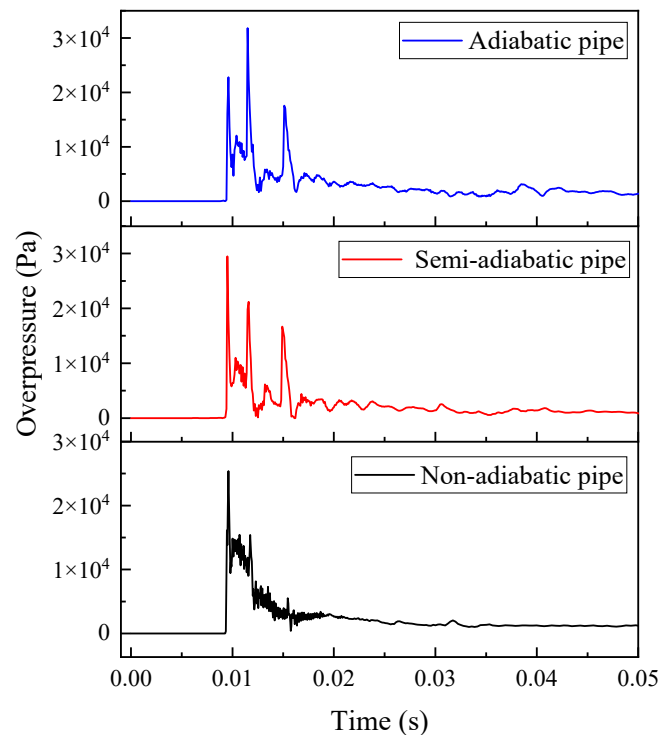


Figure 5. Cloud diagram of shock wave propagation in a pipe.



(a) Overpressure curves at different locations of non-adiabatic pipe



(b) Comparison of overpressure curves at 2.72 m for three kind of pipes

Figure 6. Overpressure curves at different locations of pipes.



The reaction process of a gas explosion releases a lot of heat and forms a high-pressure shock wave, and the high temperature and high pressure simultaneously act on the wall, resulting in huge thermal stress on the wall. The thermal stress can correspondingly reflect the intensity of the gas explosion and the energy change of the wall. Figures 7–9 show the changes in thermal stress and energy of the three pipe walls under a gas explosion. As shown in Figure 7, with the progress of the gas explosion, a large thermal stress appears on the wall under the impact of high temperature and high pressure. With the decrease in adiabatic degree, the wall heat effect increases, the heat dissipation capacity of the wall increases, the wall thermal stress decreases obviously, and the high-stress duration shortens. Compared with the adiabatic pipe, the thermal stress of the non-adiabatic pipe wall is reduced by 47.2%, and the duration is reduced by nearly half, indicating that the increase in the wall heat effect significantly weakens the gas explosion intensity.

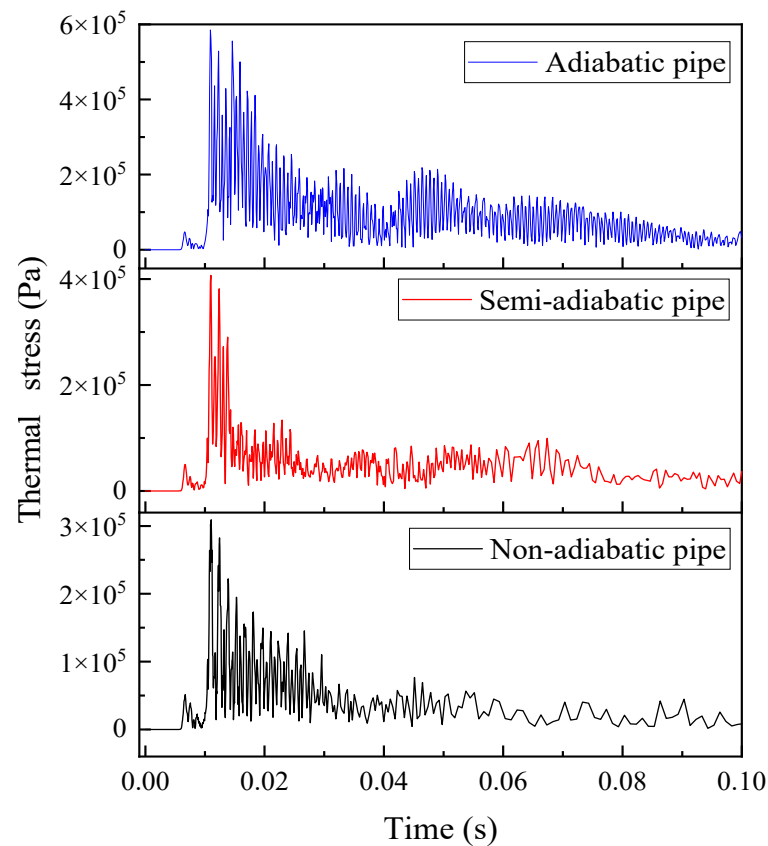
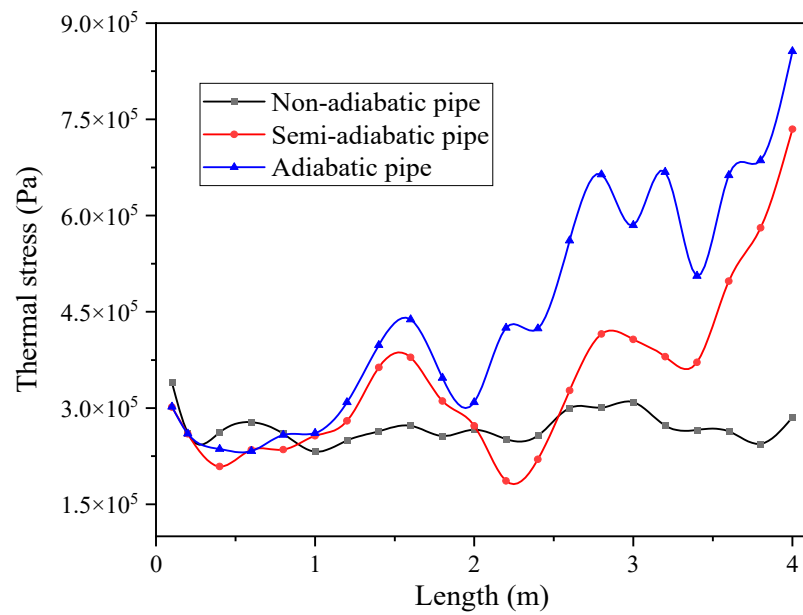
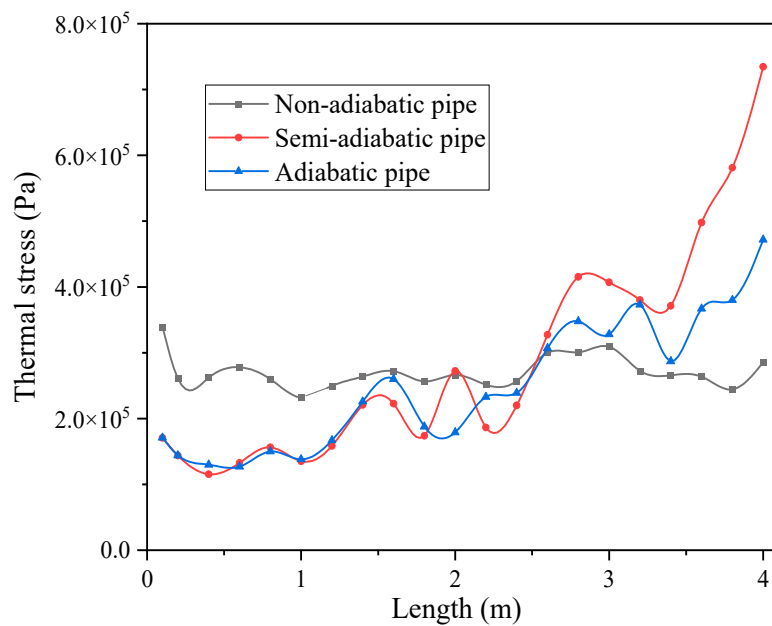


**Figure 7.** Comparison of thermal stress curves of three walls at 3m.

From Figures 8a and 9, it can be found that the thermal stress difference at the initiation section of different pipes is very small, and the thermal stress fluctuation of the non-adiabatic pipe is small. The thermal stress of the pipe wall with an adiabatic layer increases significantly after 1 m away from the ignition section. Due to the small intensity of the initial gas explosion, the thermal stress difference of different pipes is not obvious in the 1 m distance of the initial section. However, the wall heat effect of the pipe actually consumed part of the gas explosion energy, which reduces the energy of the explosion wavefront into the unburned gas and inhibits the intensity of the subsequent gas explosion reaction. The adiabatic layer reduces the wall heat effect; thus, the energy loss of the gas explosion decreases after initiation, and the energy of the explosion wavefront increases, which can cause more molecules of unburned gas to participate in the reaction, the gas explosion intensity in the pipe is greatly increased consequently. The explosion wave is continuously enhanced along the pipe, and the thermal stress of the wall is gradually increased. With the decrease in the wall heat effect, the maximum thermal stress and maximum energy of the pipe wall increase.



(a) Thermal stress of different pipe wall



(b) Thermal stress of different steel pipe

**Figure 8.** Distribution of thermal stress along the pipe.

It can be found from Figure 8b that the thermal stress of the semi-adiabatic steel pipe and the adiabatic steel pipe at a 2 m distance of the initial section is similar and is smaller than that of the non-adiabatic steel pipe, which mainly occurs the thermal stress has been significantly weakened when it passes through the adiabatic layer. In the latter 2 m, the thermal stress of semi-adiabatic steel pipe and adiabatic steel pipe exceeds that of non-adiabatic steel pipe. Due to the incomplete adiabatic layer, the maximum thermal stress of semi-adiabatic steel pipe is greater than that of adiabatic steel pipe. It indicates that the adiabatic layer enhances the explosion process more significantly. Therefore, the thermal stress of the second half of the pipe increases along the axis, and finally, the value is greater than that of the non-adiabatic pipe.

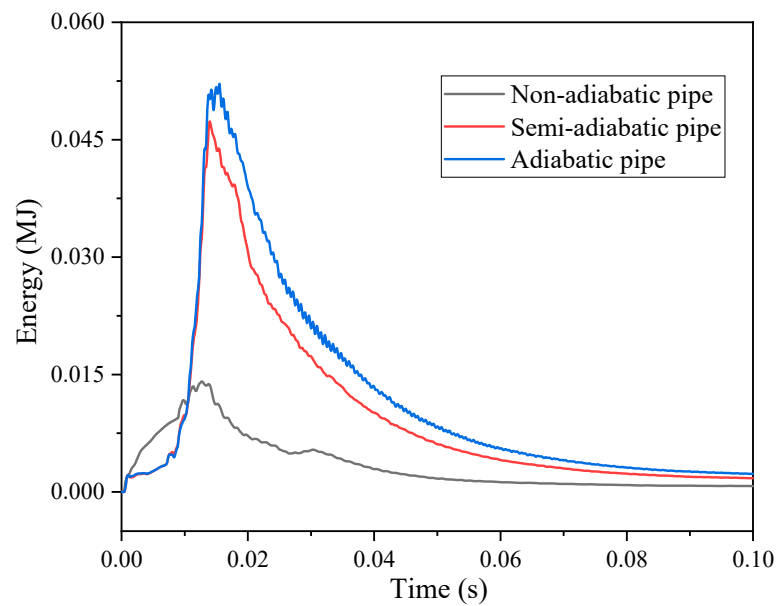


**Figure 9.** Energy change of steel pipe under gas explosion.

Based on the analysis in Figures 8b and 9, the thermal stress of the semi-adiabatic steel pipe in the middle and rear part is larger due to the incomplete adiabatic layer, but the energy transmitted to the steel pipe by a gas explosion is slightly lower than that of adiabatic steel pipe. Compared with non-adiabatic pipe, the energy of semi-adiabatic pipe and adiabatic pipe is increased by 235.3% and 269.3%, respectively. The decrease in the wall heat effect significantly improves the combustion level and energy release degree of the gas explosion process, and the energy dissipated to the wall is also greatly increased. As the wall heat effect continues to decrease, the maximum energy of the steel tube does not increase significantly, indicating that the wall heat effect has a greater impact on the gas explosion process with a high combustion level.

### 3.3. Influence of Wall Heat Effect on the Heat Release of Gas Explosion in Pipe

The gas explosion in the pipe is a very rapid heat release process, which causes the gas temperature in the pipe to rise rapidly, and forms a huge temperature difference inside and outside the pipe. Part of the heat in the pipe will spontaneously transfer outward the pipe wall along the thickness direction, forming a certain temperature gradient distribution. Figures 10–12 show the temperature distribution of different pipe walls under the wall heat effect. To make the display more intuitive and clearer, the wall near the closed end is intercepted for demonstration. It can be seen from Figure 10 that the temperature of the pipe wall increases significantly at 0.1 ms, a certain temperature gradient is formed along the thickness direction, and the temperature of the closed-end wall is higher than that of the side wall or the corner. Combined with Figure 5, it can be seen that the gas explosion has not yet spread to the closed end at this time, and the temperature rise of the wall is mainly caused by the heat radiated by the high-temperature gas in the combustion zone. Then the shock wave reaches the end of the pipe, thermal convection transfers heat from the explosion wave to the inner surface of the pipe wall, and the temperature of the pipe increases continuously. At this time, the wall temperature is determined by the thermal convection on the inner surface of the wall, the radiant heat in the combustion area, and the thermal conduction from the combusted area. The highest temperature area is transferred from the end wall to the side wall. At 1.3 ms, the temperature gradient of the pipe contacts the outer surface of the wall, and the pipe begins to dissipate heat. With the continuous action of a gas explosion, the temperature of the pipe wall rises continuously, and reaches a maximum temperature of 496 °C at 2.8 ms, then rises gradually after a small drop and reaches the second temperature peak at 10.3 ms, after which the temperature

drops continuously. These are consistent with the development law of gas explosion intensity described in Figures 4–6.

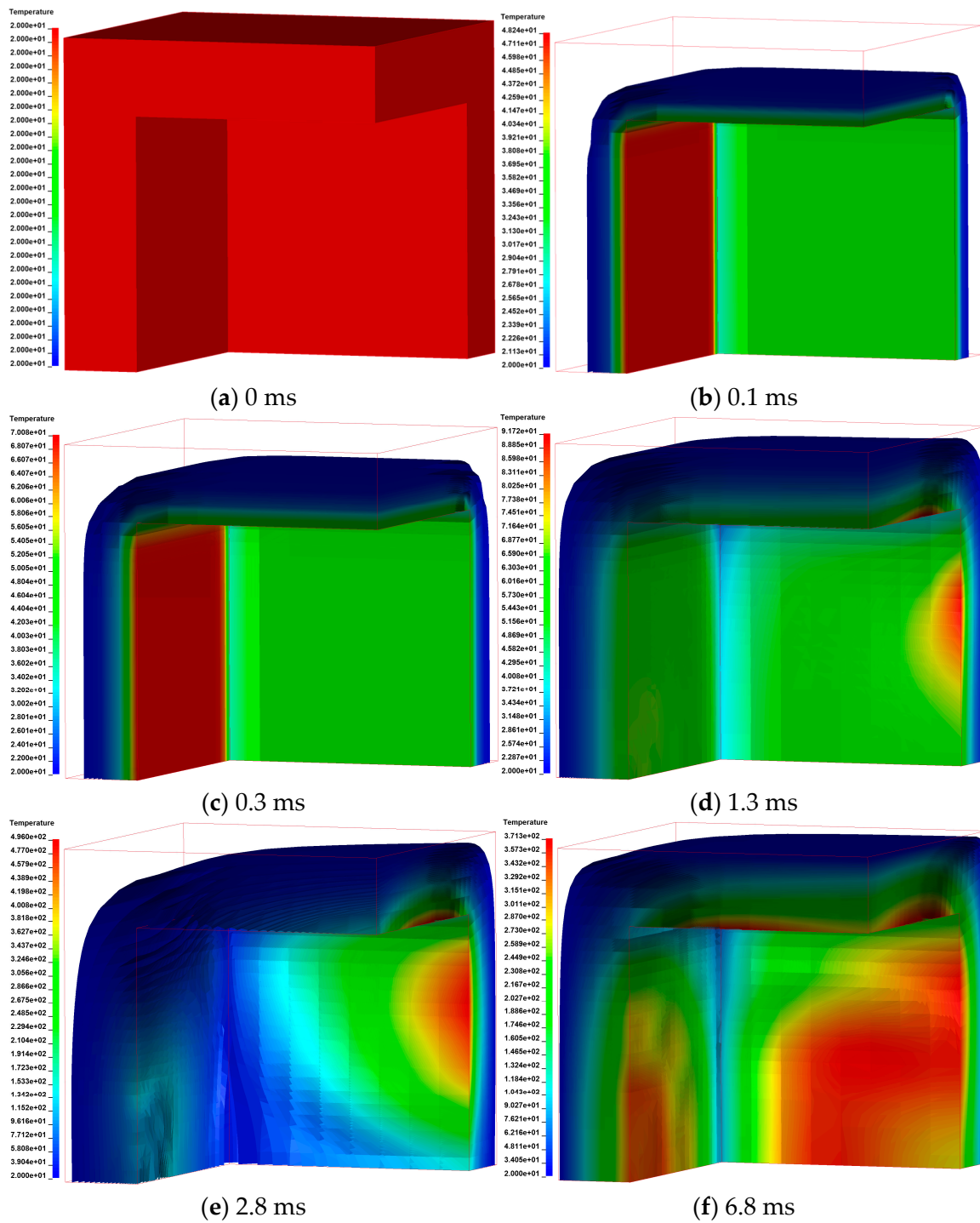
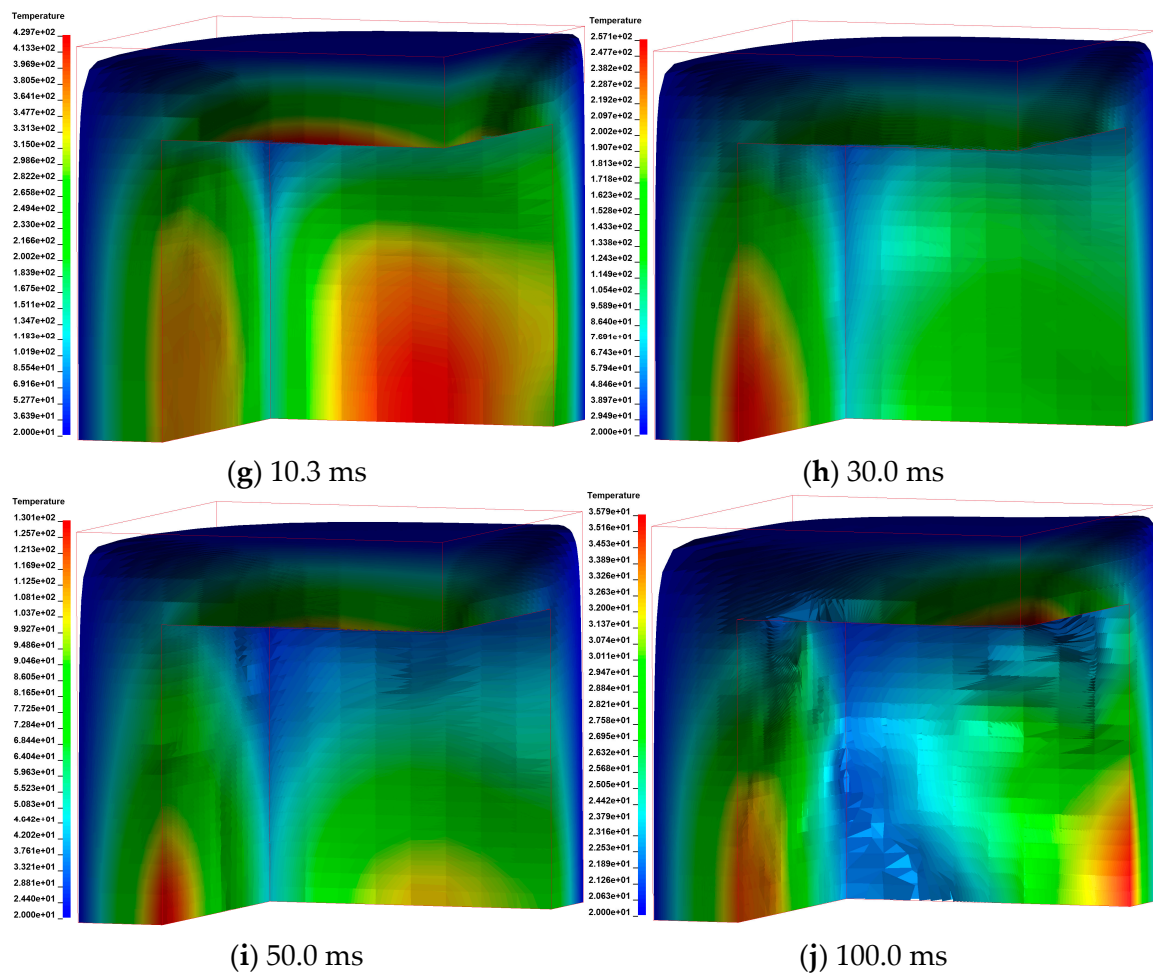


Figure 10. Cont.



**Figure 10.** Variation of temperature at the closed end of a non-adiabatic pipe.

It can be found from Figures 11 and 12 that the heat dissipation capacity of the pipe decreases with the wall heat effect decrease, the temperature difference between the inner and outer walls of the adiabatic layer is more obvious, and the temperature of the wall increases faster. The high temperature provides more activation energy for combustible gas molecules and intermediates involved in the combustion reaction and improves the gas explosion reaction rate; then, the violent chemical reactions release more heat, and the temperature in the pipe increases rapidly, forming a positive feedback of reaction acceleration. The heat generated by the reaction is continuously transferred to the closed end by thermal convection, thermal radiation, and thermal conduction in the pipe. The maximum temperature of the adiabatic pipe reaches 783 °C, which is about 1.6 times of the non-adiabatic pipe. This shows the important influence of the wall heat effect of pipe wall on the gas explosion reaction, and more severe gas explosion can occur in pipes with a higher adiabatic degree.

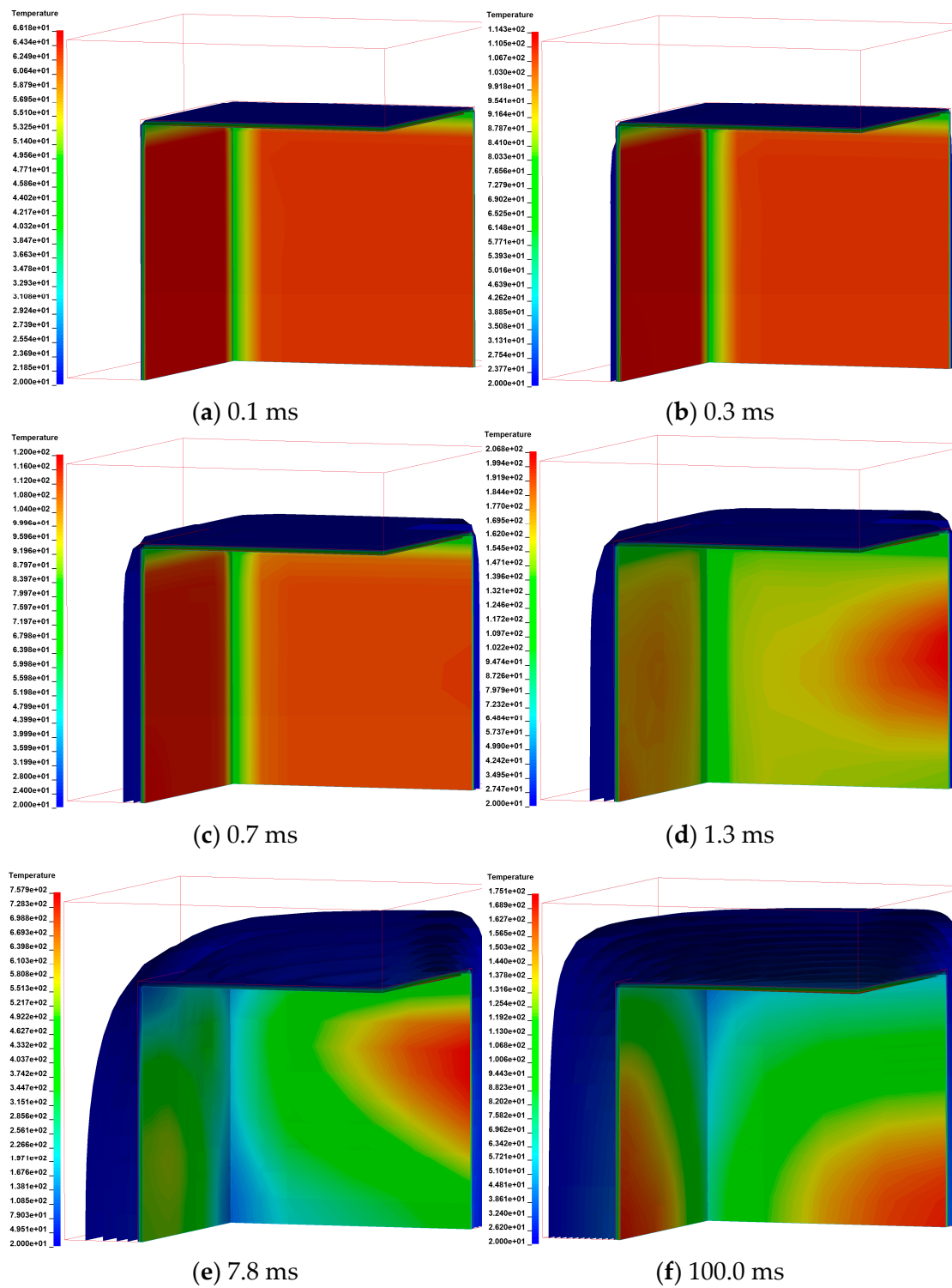
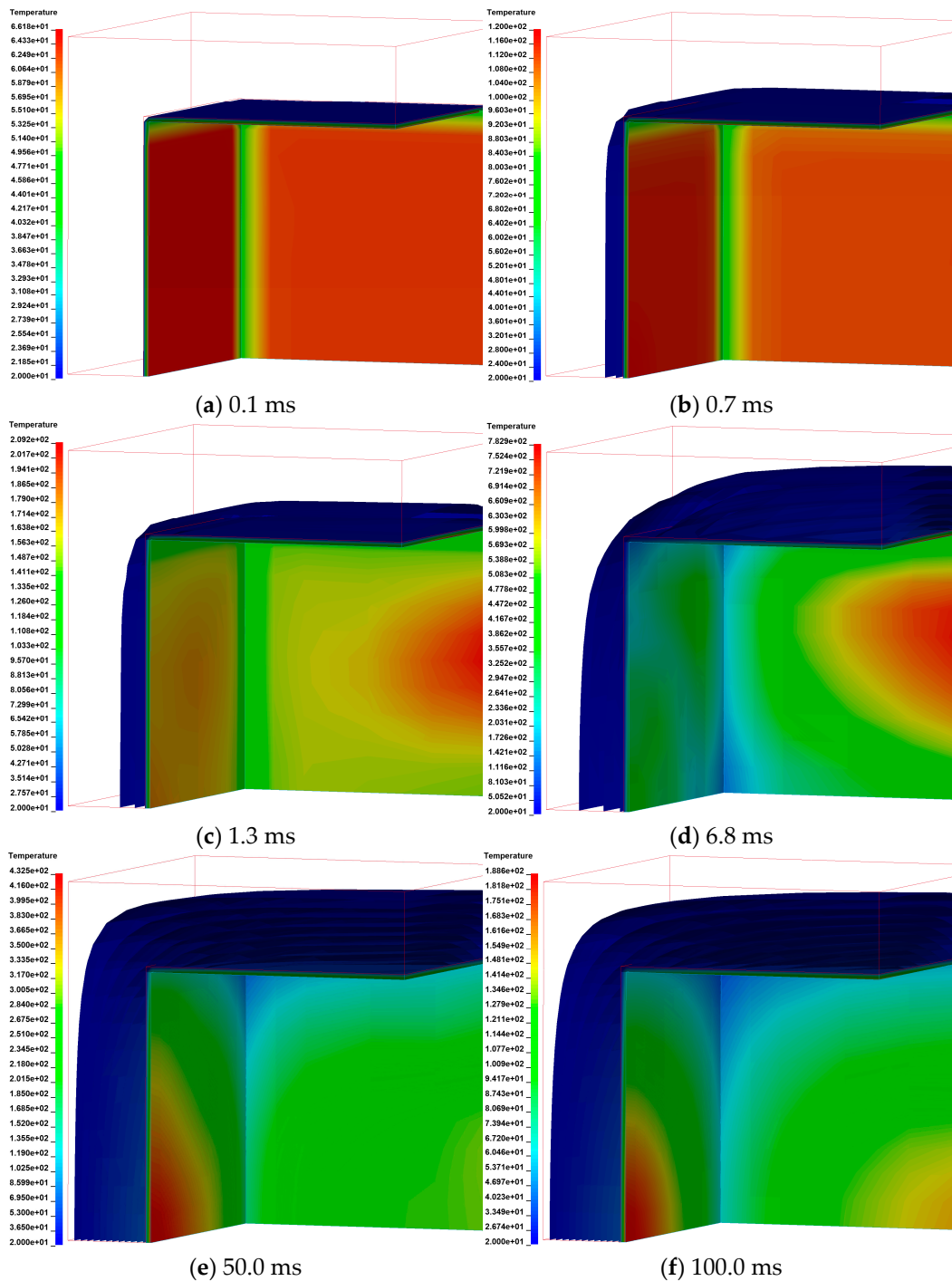


Figure 11. Variation of temperature at the closed end of a semi-adiabatic pipe.



**Figure 12.** Variation of temperature at the closed end of an adiabatic pipe.

Several measuring points are taken along the wall thickness direction at the pipe to observe the specific change in wall temperature, as shown in Figures 13 and 14. The temperature of pipes with different adiabatic degrees or different positions decreases rapidly after reaching a peak, and the temperature decreases gradually along the inner surface to the outer surface. The occurrence time of the maximum temperature is close to the time when the explosion wave burst out of the open end of the pipe, which indicates that the main reason for the rapid decline of temperature is that the explosion wave propagates out of the pipe, and the high-temperature gas is ejected from the open end to the outside environment, and the heat is quickly dissipated. The temperature change of the semi-adiabatic pipe wall fluctuates as the incomplete adiabatic layer, but the temperature

change of the non-adiabatic pipe and the adiabatic pipe is relatively smooth. As can be seen from Figure 13, the maximum temperature at the closed end of the non-adiabatic pipe is doubled from the temperature at the corner, and the maximum temperature at the closed end appears earlier. Along the thickness direction, the temperature difference is larger when closer to the outer surface. It is shown that the wall heat effect is more obvious at the end wall, and there is an important correlation between the wall heat effect and the contact area of the combustion gas-wall surface. The large contact area between the combustion gas and the wall surface is more prone to convection heat transfer and sustains more thermal radiation.

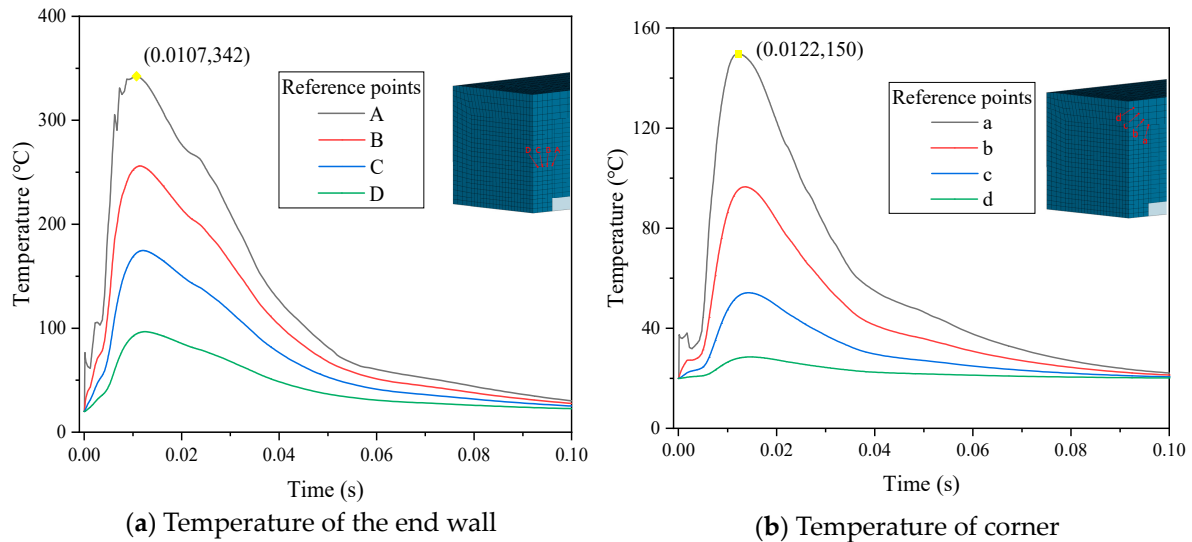


**Figure 13.** Temperature variation in the thickness direction of the closed end of non-adiabatic pipe.

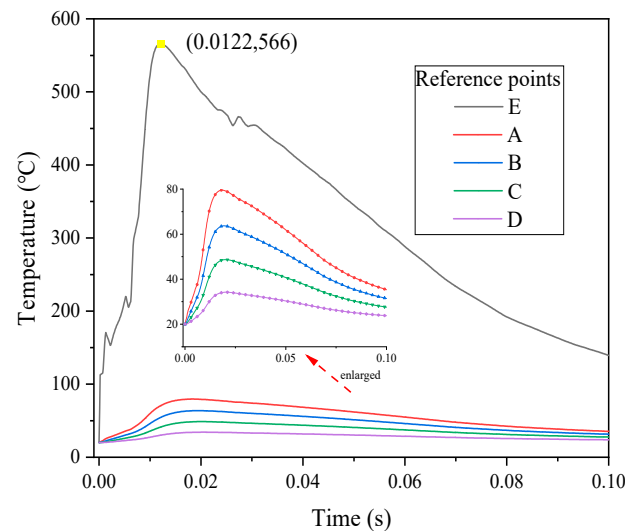


**Figure 14.** Temperature variation in the thickness direction of the closed end of adiabatic pipe.

As can be seen from Figures 14 and 15, there is a large temperature difference between the inner and outer surfaces of the asbestos layer. The temperature of the inner surface of the steel pipe is reduced to about 80 °C in the adiabatic pipe, which shows that the decrease in the wall heat effect can reduce the energy loss caused by heat dissipation of the wall. With the decrease in the wall heat effect, the temperature ratio of inner and outer walls expands from 3.54 times to 16.24 times and 16.55 times, and the peak value of pipe temperature rises from 342 °C to 549 °C and 566 °C, which shows that wall heat effect has an important influence on the gas explosion. By comparing Figures 13–15, the higher the



adiabatic degree of the pipe, the higher the maximum temperature of the wall, and the later the occurrence time. In summary, the decrease in the wall heat effect reduces the heat loss of gas explosion, and the heat is used to heat and compress the unburned gas, resulting in a more violent explosive reaction and a substantial increase in the temperature of the explosion gas.

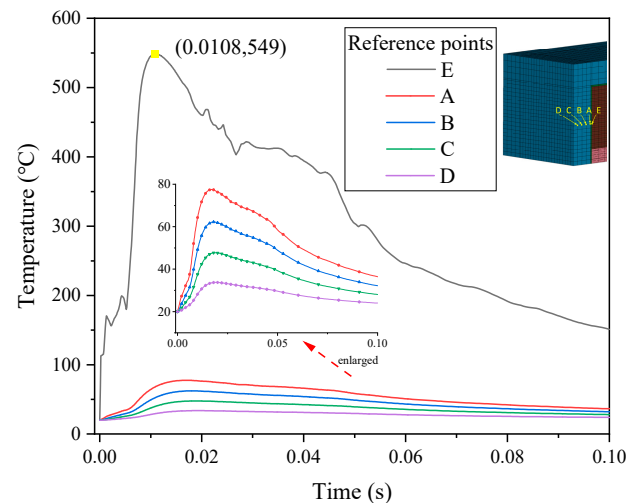


**Figure 15.** Temperature variation in the thickness direction of the closed end of semi-adiabatic pipe.

#### 4. Conclusions

In this study, the influence of wall heat effect on gas explosion and its propagation process is studied by numerical simulation, and the following conclusions are obtained:

- (1) The wall heat effect significantly reduces the intensity of the gas explosion. The wall heat effect in a semi-adiabatic pipe and non-adiabatic pipe is more serious, and the maximum explosion overpressure in the pipe is reduced by 7.3% and 20.2%, respectively. The thermal stress of the pipe wall is reduced by 30.4% and 47.2%. Compared with non-adiabatic pipe, the energy transferring to a semi-adiabatic pipe and adiabatic pipe increases by 235.3% and 269.3%, respectively. The decrease in the wall heat effect significantly increases the combustion level and energy release degree of a gas explosion, and the energy dissipated to the pipe wall increases greatly. With the wall heat effect continuing to decrease, the increase in the maximum energy of the tube decreases rapidly, which shows that the wall heat effect has more influence on the gas explosion process with high combustion level.
- (2) With the decrease in the wall heat effect, the heat dissipation ability of the pipe wall is reduced, and the temperature difference between the inner and outer walls of the pipe is enlarged. The maximum temperature of the adiabatic pipe wall is near twice that of the non-adiabatic pipe wall. The decrease in the wall heat effect enlarges the maximum temperature of the pipe, the time of occurrence is delayed, and the ratio of inner and outer wall temperature is larger. The decrease in the wall heat effect reduces the heat loss of the gas explosion, and the heat is used to heat and compress the unburned gas, which increases the explosion temperature.

The wall heat effect has a significant influence on the gas explosion and its propagation. In experiments or numerical simulations for practical conditions such as roadway gas explosion, the effect of wall heat effects on the results should be considered, and the thermal parameters of the wall should be changed accordingly. In the process industry, the wall heat effect should be considered in the design of pipes and vessels.

**Author Contributions:** Conceptualization, Z.J. and Q.Y.; methodology, Z.J. and Q.Y.; software, Z.J. and Z.Y.; investigation, Q.Y.; writing—original draft preparation, Q.Y. and Z.Y. writing—review and editing, Z.J., Q.Y. and Z.Y. All authors have read and agreed to the published version of the manuscript.

**Funding:** This work received funding from the National Natural Science Foundation Project of China (52174177, 52174178), and the project was supported by the Scientific Research Fund of the Hunan Provincial Education Department (20B240).

**Institutional Review Board Statement:** Not applicable.

**Informed Consent Statement:** Not applicable.

**Data Availability Statement:** Not applicable.

**Conflicts of Interest:** The authors declare no conflict of interest.

## References

1. Ye, Q.; Lin, B.; Jian, C.; Jia, Z.Z. Propagation characteristics of gas explosion in duct with sharp change of cross sections. *Disaster Adv.* **2012**, *15*, 999–1003.
2. Oran, E.S.; Chamberlain, G.; Pekalski, A. Mechanisms and occurrence of detonations in vapor cloud explosions. *Prog. Energy Combust. Sci.* **2020**, *77*, 100804. [[CrossRef](#)]
3. Ezekoye, O.; Greif, R.; Sawyer, R.F. Increased surface temperature effects on wall heat transfer during unsteady flame quenching. *Symp. Combust.* **1992**, *24*, 1465–1472. [[CrossRef](#)]
4. Kang, X.; Veeragavan, A. Experimental investigation of flame stability limits of a mesoscale combustor with thermally orthotropic walls. *Appl. Therm. Eng.* **2015**, *85*, 234–242. [[CrossRef](#)]
5. Ye, Q.; Jia, Z.Z.; Wang, H.; Pi, Y. Characteristics and control technology of gas explosion in gob of coal mines. *Disaster Adv.* **2013**, *6*, 112–118.
6. Jiang, B.Y.; Lin, B.Q.; Shi, S.L.; Zhu, C.J.; Jun, N. Numerical simulation on the influences of initial temperature and initial pressure on attenuation characteristics and safety distance of gas explosion. *Combust. Sci. Technol.* **2011**, *184*, 135–150. [[CrossRef](#)]
7. Frazier, C.; Lamnaouer, M.; Divo, E.; Kassab, A.; Petersen, E. Effect of wall heat transfer on shock-tube test temperature at long times. *Shock. Waves* **2011**, *21*, 211–217. [[CrossRef](#)]
8. Zhang, B.; Chang, X.; Bai, C. End-wall ignition of methane-air mixtures under the effects of CO<sub>2</sub>/Ar/N<sub>2</sub> fluidic jets. *Fuel* **2020**, *270*, 117485. [[CrossRef](#)]
9. Zhang, J.; Cheng, L.; Zheng, C.; Luo, Z.; Ni, M. Numerical studies on the inclined flame front break of filtration combustion in porous media. *Energy Fuels* **2013**, *27*, 4969–4976. [[CrossRef](#)]
10. Lei, B.; Xiao, J.; Kuznetsov, M.; Jordan, T. Effects of Heat Transfer Mechanism on Methane-Air Mixture Explosion in 20 L Spherical Device. *J. Loss Prev. Process Ind.* **2022**, *80*, 104864. [[CrossRef](#)]
11. Dai, H.; Lin, B. Scale effect of ceramic foam burner on the combustion characteristics of low-concentration coal mine methane. *Energy Fuels* **2014**, *28*, 6644–6654. [[CrossRef](#)]
12. Gao, K.; Liu, Z.; Wu, C.; Li, J.; Liu, K.; Liu, Y.; Li, S. Effect of low gas concentration in underground return tunnels on characteristics of gas Explosions. *Process Saf. Environ. Prot.* **2021**, *152*, 679–691. [[CrossRef](#)]
13. Wang, L.Q.; Ma, H.H.; Shen, Z.W. An experimental investigation on explosion behaviors of syngas-air mixtures in a vessel with a large blockage ratio perforated plate. *Fuel* **2020**, *264*, 116842. [[CrossRef](#)]
14. Sun, Z.Y.; Li, G.X. Turbulence influence on explosion characteristics of stoichiometric and rich hydrogen/air mixtures in a spherical closed vessel. *Energy Convers. Manag.* **2017**, *149*, 526–535. [[CrossRef](#)]
15. Huang, K.; Sun, Z.; Tian, Y.-C.; Wang, K.-L. Turbulent combustion evolution of stoichiometric H<sub>2</sub>/CH<sub>4</sub>/air mixtures within a spherical space. *Int. J. Hydrogen Energy* **2019**, *45*, 10613–10622. [[CrossRef](#)]
16. Zhang, Q.H.; Duan, Y.L.; Zhou, X.Q.; Tang, H.Y.; Qin, M.G. Special thermal environment of adjacent explosions center areas after methane explosions. *J. China Coal Soc.* **2011**, *36*, 1165–1171. [[CrossRef](#)]
17. Duan, Y.; Yu, M.; Yao, X.; Pei, B.; Wang, H. Study on spatial temperature distribution and thermal hazard area analysis after gas explosion. *J. Saf. Sci. Technol.* **2018**, *14*, 56–62. [[CrossRef](#)]
18. Ye, Q.; Jia, Z.; Zheng, C. Study on hydraulic-controlled blasting technology for pressure relief and permeability improvement in a deep hole. *J. Pet. Sci. Eng.* **2017**, *159*, 433–442. [[CrossRef](#)]
19. Chen, X.F.; Zhang, J.H.; Wang, Y.J.; Ren, S.F. Experimental study of flame microstructure and propagation behavior of mine-gas explosion. *J. Coal Sci. Eng.* **2008**, *14*, 550–553. [[CrossRef](#)]
20. Yang, Z.; Ye, Q.; Jia, Z.; Li, H. Numerical simulation of pipeline-pavement damage caused by explosion of leakage gas in buried PE pipelines. *Adv. Civ. Eng.* **2020**, 4913984. [[CrossRef](#)]
21. Salzano, E.; Cammarota, F.; Di Benedetto, A.; Di Sarli, V. Explosion Behavior of Hydrogen–Methane/Air Mixtures. *J. Loss Prev. Process Ind.* **2012**, *25*, 443–447. [[CrossRef](#)]
22. Ye, Q.; Jia, Z.Z. Effect of the bifurcating duct on the gas explosion propagation characteristics. *Combust. Explos. Shock. Waves* **2014**, *50*, 424–428. [[CrossRef](#)]
23. Campbell, A.N. The effect of external heat transfer on thermal explosion in a spherical vessel with natural convection. *Phys. Chem. Chem. Phys.* **2015**, *17*, 16894–16906. [[CrossRef](#)]
24. Yan, Y.; Wang, H.; Pan, W.; Zhang, L.; Li, L.; Yang, Z.; Lin, C. Numerical study of effect of wall parameters on catalytic combustion characteristics of CH<sub>4</sub>/air in a heat recirculation micro-combustor. *Energy Convers. Manag.* **2016**, *118*, 474–484. [[CrossRef](#)]

25. Ye, Q.; Wang, G.X.; Jia, Z.; Zheng, C. Experimental study on the influence of wall heat effect on gas explosion and its propagation. *Appl. Therm. Eng.* **2017**, *118*, 392–397. [[CrossRef](#)]
26. Liu, T.Y.; Campbell, A.N.; Hayhurst, A.N.; Cardoso, S.S.S. On the occurrence of thermal explosion in a reacting gas: The effects of natural convection and consumption of reactant. *Combust. Flame* **2010**, *157*, 230–239. [[CrossRef](#)]
27. Du, Y.; Zhou, F.; Ma, L.; Zheng, J.; Xu, C.; Chen, G. Consequence analysis of premixed flammable gas explosion occurring in pipe using a coupled fluid-structure-fracture approach. *J. Loss Prev. Process Ind.* **2019**, *57*, 81–93. [[CrossRef](#)]
28. Zhang, J.; Zhang, L.; Liang, Z. Buckling failure of a buried pipeline subjected to ground explosions. *Process Saf. Environ. Prot.* **2017**, *114*, 36–47. [[CrossRef](#)]
29. Ma, Q.J.; Zhang, Q.; Pang, L. Influence of the tunnel wall surface condition on the methane-air explosion. *Combust. Explos. Shock. Waves* **2014**, *50*, 208–213. [[CrossRef](#)]
30. Di Sarli, V.; Cammarota, F.; Salzano, E. Explosion Parameters of Wood Chip-Derived Syngas in Air. *J. Loss Prev. Process Ind.* **2014**, *32*, 399–403. [[CrossRef](#)]
31. Shamsuddin, D.S.N.A.; Fekeri, A.F.M.; Muchtar, A.; Khan, F.; Khor, B.C.; Lim, B.H.; Rosli, M.I.; Takriff, M.S. Computational Fluid Dynamics Modelling Approaches of Gas Explosion in the Chemical Process Industry: A Review. *Process Saf. Environ. Prot.* **2023**, *170*, 112–138. [[CrossRef](#)]

**Disclaimer/Publisher’s Note:** The statements, opinions and data contained in all publications are solely those of the individual author(s) and contributor(s) and not of MDPI and/or the editor(s). MDPI and/or the editor(s) disclaim responsibility for any injury to people or property resulting from any ideas, methods, instructions or products referred to in the content.